From Kosterlitz-Thouless to Pokrovsky-Talapov transitions in spinless fermions and spin chains with next-nearest-neighbor interactions

Natalia Chepiga
Kavli Institute of Nanoscience, Delft University of Technology, Lorentzweg 1, 2628 CJ Delft, The Netherlands

(Received 22 September 2022; revised 31 October 2022; accepted 7 December 2022; published 30 December 2022)

We investigate the nature of the quantum phase transition out of density-wave phase in a spinless fermion model with nearest- and next-nearest-neighbor interaction at one-third filling. Using extensive density matrix renormalization group (DMRG) simulations, we show that the transition changes it nature. For weak next-nearest-neighbor coupling the transition is of Kosterlitz-Thouless type, in agreement with bosonisation predictions. For large next-nearest-neighbor repulsion we provide numerical evidences that the transition belongs to the Pokrovsky-Talapov univerality class describing a nonconformal commensurate-incommensurate transition. We argue that the change of the nature of the transition is a result of incommensurability induced by frustration and realized even at zero doping. The implications in the context of the XXZ chain with next-nearest-neighbor Ising interaction is briefly discussed.

DOI: 10.1103/PhysRevResearch.4.043225

I. INTRODUCTION

Understanding the nature of quantum phase transitions in low-dimensional systems is one of the central topics in condensed matter physics[1–3]. The conjecture of universality classes allows to investigate phase transitions on a simple lattice models. A paradigmatic example that appeared in many contexts over the decades is a model of interacting spinless fermions in one dimension [1]. Their applications ranged from solving spin models through Jordan-Wigner transformation [4] to studying the commensurate melting of classical two-dimensional (2D) and later quantum one-dimensional (1D) models [5–11]. The models with competing nearest-neighbor (NN) and next-nearest-neighbor (NNN) interactions has been studied intensely over the years [12–16]. Initially formulated as a toy model for the long-range Coulomb interaction, it was soon realized that, despite its simplicity, the model has very rich phase diagram hosting, in particular the Luttinger liquid phase, the density waves at half- and third-fillings, and paired phases [16–18]. The full phase diagram, however, is far from being complete and there are a number of questions that remain open. For instance, the properties of the highly entropic phase reported recently [16] or the nature of quantum phase transitions that will be the main focus of this paper. Our analysis is based on the combination of field theory predictions in 1 + 1D [19–22] and the density matrix renormalization group algorithm (DMRG) [23–26] that, over the past decades, has proven to be extremely powerful in coming up with theoretical predictions for numerous fascinating critical phenomena.

In this paper we investigate the nature of the quantum phase transition between the density wave phase realized at one-third filling and the Luttinger liquid phase for a chain of spinless fermions with nearest-neighbor and next-nearest-neighbor repulsion. The microscopic model is defined by the following Hamiltonian:

$$H_{\text{ferm}} = \sum_i -t(c_i^\dagger c_{i+1} + \text{H.c.}) + U_1 n_i n_{i+1} + U_2 n_i n_{i+2}, \quad (1)$$

where $c_i^\dagger$, c_i are fermionic creation and annihilation operators, t is a hoping amplitude, and $U_{1,2}$ are nearest-neighbor and next-nearest-neighbor coupling constants, correspondingly. The model can be reformulated in terms of hard-core bosons and the Hamiltonian takes essentially the same form. By means of Jordan-Wigner transformation the model can also be rewritten in terms of spin-1/2 operators with the following Hamiltonian:

$$H_{\text{spin}} = \sum_i -t(S_i^+ S_{i+1}^- + S_i^- S_{i+1}^+) + U_1 S_i^z S_{i+1}^z + U_2 S_i^z S_{i+2}^z, \quad (2)$$

where $S_i^\pm = S_i^x \pm i S_i^y$. The Hamiltonian of Eq. (1) preserves the total number of fermions, while in the spin version of the Hamiltonian of Eq. (2) the total magnetization is conserved. It is, therefore, natural to study the phase diagram of these models at a fixed filling or fixed magnetization. Here we will focus on one-third filling. In the spin language this corresponds to the total magnetization $S_{\text{tot}}^z = -(N-1)/6$ [27] and the ground state of the form $\uparrow\downarrow\downarrow$. Since the Hamiltonian obeys particle-hole symmetry our results will also be valid for two-third filling.

In the noninteracting case $U_1 = U_2 = 0$ the ground state can be described by the Luttinger liquid with the Luttinger liquid parameter $K = 1$. Repulsive interactions do not immediately destroy the Luttinger liquid leading to a critical phase with $K < 1$. At one-third filling a large portion of the phase diagram is occupied by the density wave phase that

spontaneously breaks translation symmetry with every third site occupied by a fermion [16]. According to the theory of Mott-U transitions [7], i.e., those that take place as a function of coupling while the filling is fixed, one can expect the transition between the density-wave phase and the Luttinger liquid phase to be of the Kosterlitz-Thouless type [21]. According to bosonisation, this transition takes place when the Luttinger liquid parameter reaches the critical value $K^c = 2/9$ [16]. But how robust is this prediction against strong next-nearest-neighbor coupling? And how robust is the prediction of the Kosterlitz-Thouless transition in general against multiple competing interactions and frustration?

Recently, it was shown that the Luttinger liquid phase can be stabilized for a model with strong nearest-neighbor and next-nearest-neighbor repulsion up to the Luttinger liquid parameter $K^c = 1/9$. The result is exact in the limit of the NNN blockade [28], but it is expected to hold even for large-enough but finite interaction strength [29]. In this case the transition out of the density-wave phase belongs to the Pokrovsky-Talapov universality class [22]. The stability of the Luttinger liquid was studied as a function of chemical potential μ, which in Giamarchi's notations [7] corresponds to the Mott-δ transition, i.e., the one that takes place at a fixed coupling constant while the filling is tuned by μ. However, this raises two interesting questions: (i) Whether the Luttinger liquid phase for strong NNN repulsion is stable up to $K^c = 1/9$ also for the fixed one-third filling and (ii) whether such an extension of the Luttinger liquid phase beyond $K^c_{\mathrm{KT}} = 2/9$ in turn leads to a different type of quantum phase transition to the period-3 phase?

In this paper we show that the nature of the quantum transition out of the period-three phase changes from the Kosterlitz-Thouless type realized for weak coupling U_2 to the Pokrovsky-Talapov universality class that appears for strong U_2 as shown in Fig. 1. We argue that incommensurability associated with Pokrovsky-Talapov transition is a result of a frustration induced by the repulsion and a filling constraint. This results in the appearance of the floating phase — a region of the Luttinger liquid phase with the local density in the finite-size system oscillating around its fixed value 1/3 with the wave vector noticeably different from the commensurate value $q = 2\pi/3$.

The rest of the paper is organized as follows. In Sec. II we provide technical details of the used numerical method. In Sec. III we numerically verify the prediction for Kosterlitz-Thouless transition for small U_2. In Sec. IV we provide numerical evidences for the Pokrovsky-Talapov transition and demonstrate the emergence of the incommensurate floating phase. Finally, in Sec. V we summarize the results and put them into perspective.

II. NUMERICAL METHOD

Numerical simulations were performed with the density matrix renormalization group (DMRG) algorithm [23–26] for the spin model of Eq. (2). Without loss of generality the hopping amplitude is set to $t = 1$ throughout the paper. The results are obtained for chains with up to $N = 3601$ sites with open boundary conditions, keeping up to $D = 3000$ states and discarding singular values below 10^{-8}. This allows to converge the ground-state energy with the error well below 10^{-7}. Thus high accuracy turns out to be a prerequisite to observe the floating phase on a finite-size chains with $N = 301$ and 601 sites (see, for instance, Fig. 5). To realize 1/3 filling of the fermionic model, the algorithm is constrained to the sector with total magnetization $S^z_{\mathrm{tot}} = -(N-1)/6 + 1/2$ with $N = 3k + 1$, $k \in \mathbb{Z}$. The boundary conditions are fixed by polarizing the edge spins in the z-direction.

Most of the results were obtained with quantities that do not depend on the statistics. The correlation length ξ is extracted inside the gapped period-three phase by fitting an exponential decay of the correlation function $\langle S^z_i S^z_j \rangle$. Up to a constant this is equivalent to density-density correlations $\langle n_i n_j \rangle$ in the fermion model. The Luttinger liquid parameter

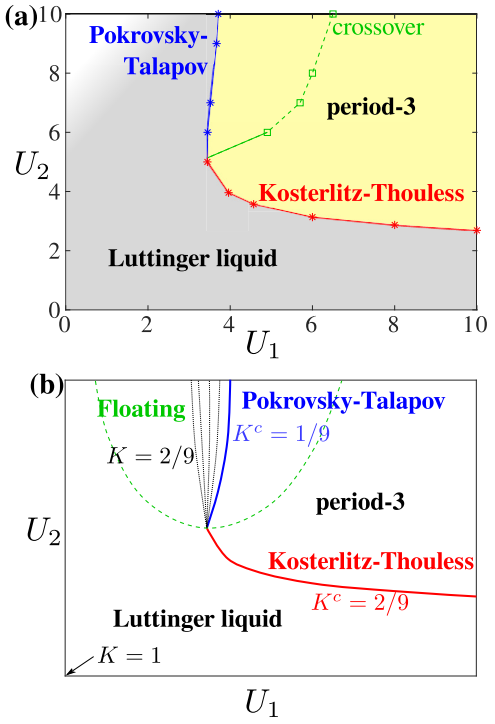

FIG. 1. Phase diagram as a function of nearest-neighbor and next-nearest-neighbor repulsion for the one-third filling. (a) Phase diagram obtained with DMRG simulations. For $U \lesssim 5$ the transition is in the Kosterlitz-Thouless universality class (red); for $U \gtrsim 5$ the transition is of Pokrovsky-Talapov type (blue). Green squares mark the location of the kinks in the correlation length, dashed green line is a guide to eyes. White region corresponds to the possible highly entropic phase [16], which is out of the scope of the present study. (b) Schematic sketch of the main features of the Luttinger liquid phase on the phase diagram presented in (a). The Luttinger liquid parameter is $K = 1$ at $U_1 = U_2 = 0$ and decreases upon approaching the boundary of the period-three phase. At the Kosterlitz-Thouless transition the K takes the critical value $K^c = 2/9$. At the Pokrovsky-Talapov transition the corresponding critical value is $K^c = 1/9$. Equal-K lines with $1/9 < K < 2/9$ (black dotted lines) are expected to collapse at the point where the transition changes its nature. The crossover line (green dashed) is expected to continue in the critical phase separating the commensurate Luttinger liquid form the floating phase with incommensurate wave-vector q. Location of the commensurate-incommensurate crossover in the Luttinger liquid phase is unknown, green dashed line is just indicative.

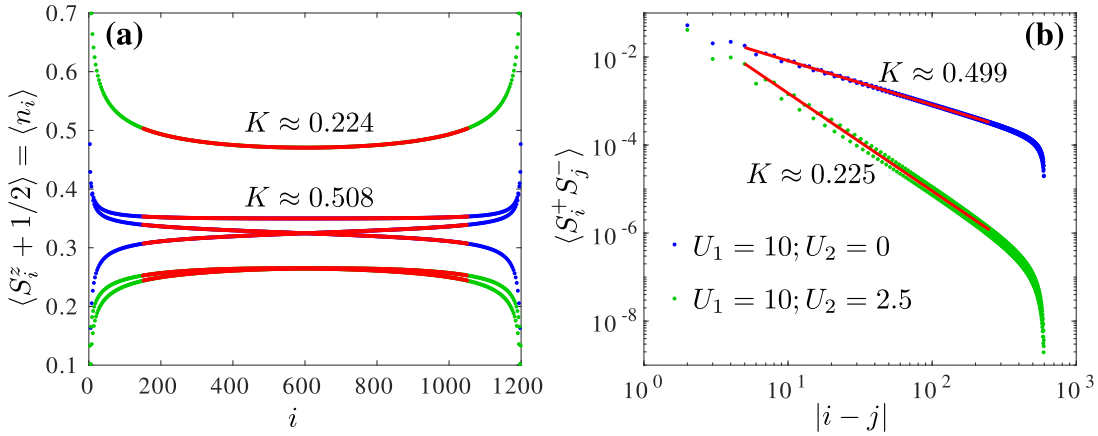

FIG. 2. Extraction of the Luttinger liquid exponent K by fitting (a) the Friedel oscillations of the local density on a finite chain and (b) the transverse component of the spin-spin correlations. The results are shown for $U_1 = 10$ at $U_2 = 0$ (blue) and at $U_2 = 2.5$ (green) (in the thermodynamic limit the critical point is located at $U_2 \approx 2.462$). The results of the fit are shown in red.

K is extracted by fitting the profile of the local magnetization $\langle S_i^z \rangle$. This is equivalent to the local density profile $\langle n_i \rangle$. Fixed boundary conditions act as an impurity and lead to Friedel oscillations. According to the boundary conformal field theory the profile takes the following form [30]:

$$S_j^z \propto \frac{\cos(qj)}{[(N/\pi)\sin(\pi j/N)]^K}. \tag{3}$$

One can benchmark the value of the Luttinger liquid exponent K obtained with Friedel oscillations by comparing it to the slope of the correlation function of the transverse components of spins $\langle S_i^+ S_j^- \rangle$. This is the only statistics sensitive quantity used in this paper. This correlation function is much easier to compute and to fit in the spin language than in the fermionic one. Figure 2 provides some examples of the fits. In general the two methods give similar results and from now on we only present the results obtained with Friedel oscillations. The error bars are estimated by fitting different intervals of the data points discarding from 5% to 25% of the spins at each edge.

Finally, the incommensurate wave-vector q was obtained by fitting the Friedel oscillations inside the floating phase.

III. KOSTERLITZ-THOULESS TRANSITION

Let us first focus on the Kosterlitz-Thouless transition and let us start with the line $U_1 = U_2$. The results for the Luttinger liquid exponent K extracted by fitting the Friedel oscillations are presented in Fig. 3(a). In the noninteracting case the well-known result $K = 1$ is recovered. Away from this point the Luttinger liquid exponent decreases in agreement with the repulsive interactions in the system. Close to the transition finite-size effects becomes stronger. Note that, due to the exponential divergence of the correlation length typical for the Kosterlitz-Thouless transition, one can extract an effective Luttinger liquid exponent even beyond the transition; this effective exponent is expected to decay to zero in the thermodynamic limit.

To locate the critical point in the thermodynamic limit we first locate the point where the curve $K(U_2)$ for each system size N crosses the line $K^c = 2/9$ and then extrapolate the obtained values with a quadratic [31] fit in $1/N$ as shown in Fig. 3(b). The correlation length is computed by fitting exponential decay of the density-density correlations in the period-three phase. At the Kosterlitz-Thouless transition the correlation length is expected to diverge as $\xi \propto \exp[A/\sqrt{U - U^c}]$ [21], where A is some nonuniversal constant. Figure 3(c) presents the inverse of the correlation length upon approaching the transition. In Fig. 3(d) the correlation length is shown as a function of a square root of a distance to the transition in a semi-log scale. One can see that the scaling systematically approaches the straight line in agreement with the theory prediction.

The results along the cut at $U_1 = 10$ are organized in a similar way and presented in Figs. 3(e) to 3(h). Similar to the previous case one can see a good agreement between numerical data and the expected exponential divergence of the correlation length. These results confirm that for small values of U_2 the transition belongs to the Kosterlitz-Thouless universality class and that the Luttinger liquid exponent takes the value $K^c_{\mathrm{KT}} = 2/9$ at the transition.

IV. POKROVSKY-TALAPOV TRANSITION

Let us now take a look at the boundary of the same period-three phase but for large values of U_2. From Figs. 4(a) to 4(b) one can see that the inverse of the correlation length upon approaching the transition vanishes with an infinite slope in a striking difference to the Kosterlitz-Thouless transition with the exponentially diverging correlation length presented in Figs. 3(c) and 3(g). We fit the data points with $1/\xi \propto (U_1 - U_1^c)^\nu$, where ν is the correlation length critical exponent that takes very special value $\nu = 1/2$ at the Pokrovsky-Talapov transition [22]. The fits are in spectacular agreement with the numerical data, especially given that there are only two fitting parameters: the location of the critical point U_1^c and the prefactor. Slight shift of the critical point is a typical finite-size effect [30,32].

Pokrovsky-Talapov transition is a commensurate-incommensurate transition and the natural question that arises at this stage is how the incommensurability appears in the phase diagram with the fixed commensurate filling? By looking at the correlation length further away from the

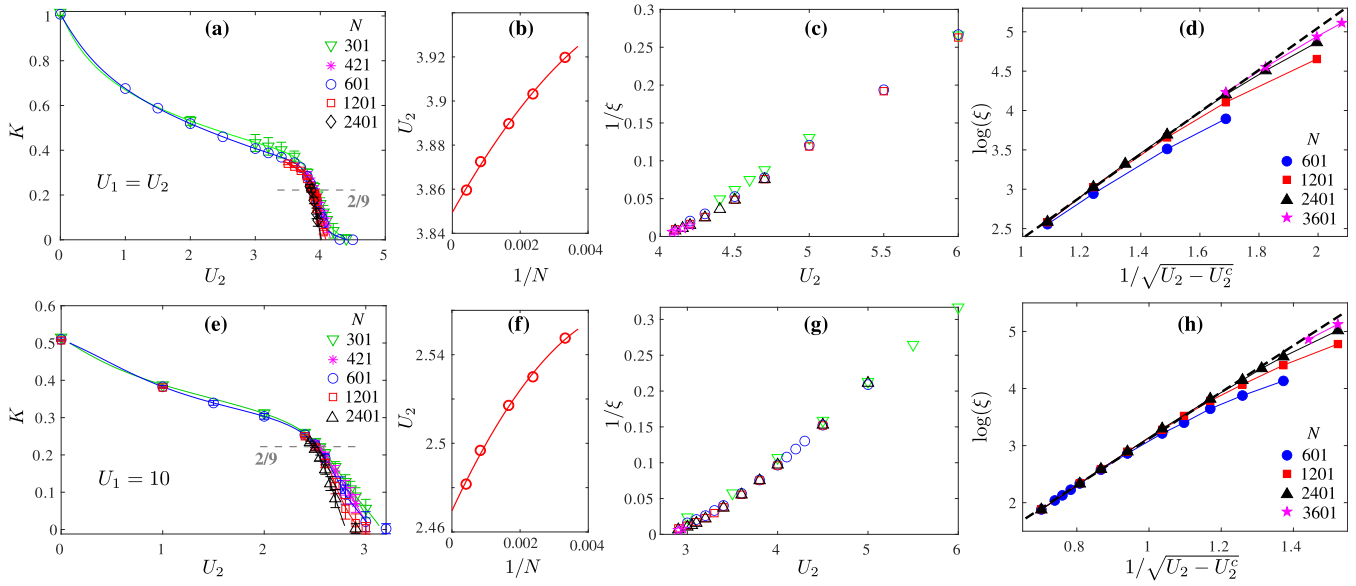

FIG. 3. Numerical results for the Kosterlitz-Thouless transition along (a)–(d) $U_1 = U_2$ diagonal cut and (e)–(h) $U_1 = 10$ vertical cut. (a,e) Effective values of the Luttinger liquid parameter K extracted by fitting finite-size Friedel oscillation profiles. (b,f) Finite-size extrapolation of the location of the finite-size critical point associated with $K^c = 2/9$ towards the thermodynamic limit. Red circles are data, solid lines are polynomial in $1/N$ fits. Extrapolated critical values are (a) $U_1^c = U_2^c \simeq 3.849$ and (f) $U_1 = 10$, $U_2^c \simeq 2.469$. (c,g) Inverse of the correlation length extracted from the density-density correlations in the period-three phase. (d,h) Exponential divergence of the correlation length in the period-three phase as a function of a distance to the transition. Dashed lines are linear fit of (b) five and (c) seven points the farthest from the transition for $N = 2401$.

transition one can notice a pronounced kink. Typically, when there is no constraint on the filling, such kinks signal the disorder line separating commensurate and incommensurate regimes. Inside the period-three phase, however, the fixed fillings as well as the long-range order of the gapped phase force the dominant wave vector to be commensurate $q = 2\pi/3$. Within the numerical precision obtained results always agree with this value. Interestingly, if one keeps track of the location of the kink, it turns out that the line crosses the boundary of the period-3 phase at $U_2 \approx 5$ as shown in Fig. 1. This agrees with the point where the transition changes its nature.

It is natural to expect the crossover line to continue in the critical phase where it will separates commensurate Luttinger liquid from the floating phase as sketched in Fig. 1(b). In the critical phase the appearance of the incommensurability can be captured explicitly. Figure 5 provides a few examples of the Friedel oscillations profile where the local density fluctuates around $n = 1/3$ with the wave vector noticeably different from $2\pi/3$. For the model written in terms of spin operators in Eq. (2) it is easy to see that all next-nearest-neighbor bonds cannot be simultaneously minimized for the imposed total magnetization $S^z_{\rm tot} = -(N-1)/6$ with commensurate period-3 configuration $\uparrow\downarrow\downarrow$. The incommensurate fluctuations of local density presented in Fig. 5 appear as a response to this frustration and give rise to a commensurate-incommensurate nature of the Pokrovsky-Talapov transition at large U_2.

By fitting the Friedel oscillations profile as shown in Fig. 5 one can get an accurate estimate of the

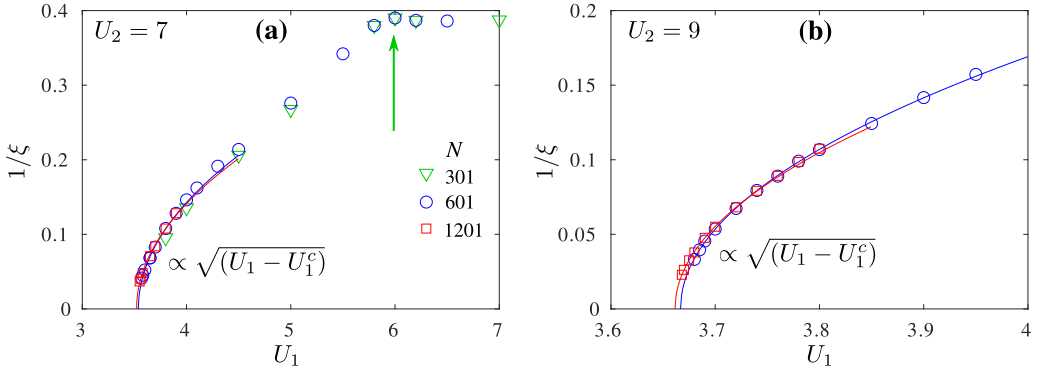

FIG. 4. Inverse of the correlation length upon approaching the transition from the period-three phase along (a) $U_2 = 7$ and (b) $U_2 = 9$. Symbols are numerical data, lines are fits with $1/\xi \propto (U - U_c)^\nu$ with the Pokrovsky-Talapov critical exponent $\nu = 1/2$. In (a) one can see the appearance of pronounced kinks indicated with green arrows. The location of the kink corresponds to green squares on the phase diagram of Fig. 1.

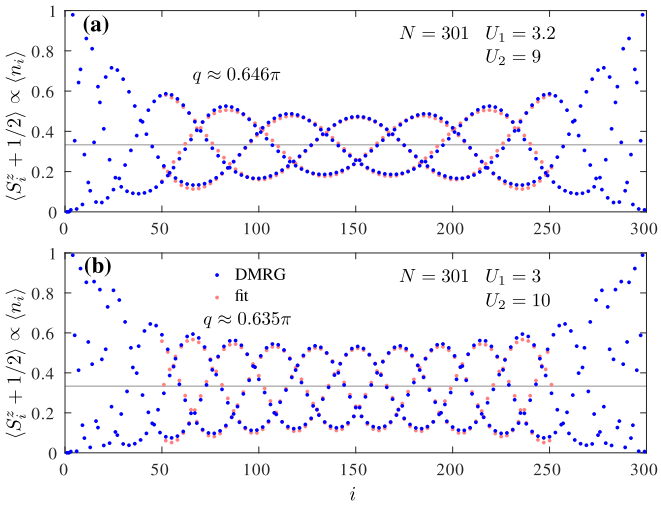

FIG. 5. Examples of the local density profiles inside the Luttinger liquid phase for large values of U_2. Competition between the one-third filling constraint and next-nearest-neighbor interaction lead to incommensurate oscillations of the local density around the fixed value 1/3 (gray line). The DMRG data are shown in blue, the results of the fit are shown in pink, an incommensurate wave-vector q obtained from the fit is indicated at each panel.

incommensurate wave-vector q. The results for $U = 9$ are summarized in Fig. 6. The error bars are estimated as $\delta q \approx \pi/N$ — the elementary value of the wave vector that on the entire chain with N sites accumulates into one turn by π. At the Pokrovsky-Talapov [22] transition the wave-vector q is expected to approach its commensurate value with the critical exponent $\bar{\beta} = 1/2$. The obtained numerical data are fit with $\Delta q \propto (U_1^c - U)^{1/2}$, where the location of the critical point is fixed to the value extracted from the fit of the correlation length for $N = 1201$ [see Fig. 4(b)]; so the only fitting parameter for Δq is the nonuniversal prefactor. The numerical data are in spectacular agreement with this theory prediction. Numerical data for other cuts through the Pokrovsky-Talapov transition can be found in the Appendix.

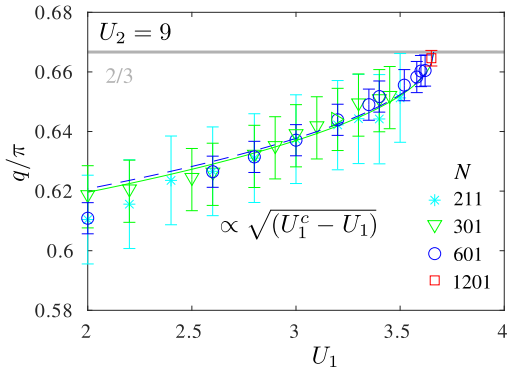

FIG. 6. Incommensurate wave-vector q as a function of U_1 upon approaching the Pokrovsky-Talapov transition. Numerical data (symbols) agree with the theory prediction (lines) $q - 2\pi/3 \propto (U_1^c - U_1)^{\bar{\beta}}$ with the Pokrovsky-Talapov critical exponent $\bar{\beta} = 1/2$. Green line shows the result of the fit for $N = 301$ and dashed blue line states for $N = 601$. For the fits U_1^c is fixed to the value obtained in Fig. 4(b) for $N = 1201$ sites.

V. DISCUSSION

To summarize, the nature of the quantum phase transition of the fermionic chain with nearest-neighbor and next-nearest-neighbor interactions changes from the Kosterlitz-Thouless type realized for small U_2 to the Pokrovsky-Talapov commensurate-incommensurate transition realized when U_2 is strong. Incommensurate oscillations appears in the Luttinger liquids ubiquitously by tuning the total density with the chemical potential [7–11,29,33]. In the present model we witness a different mechanism — an incommensurability appears due to a competition between the next-nearest-neighbor repulsion and the imposed constraint on the filling. This opens new possibilities in the theory of Mott-U transitions in the presence of competing interactions or frustration.

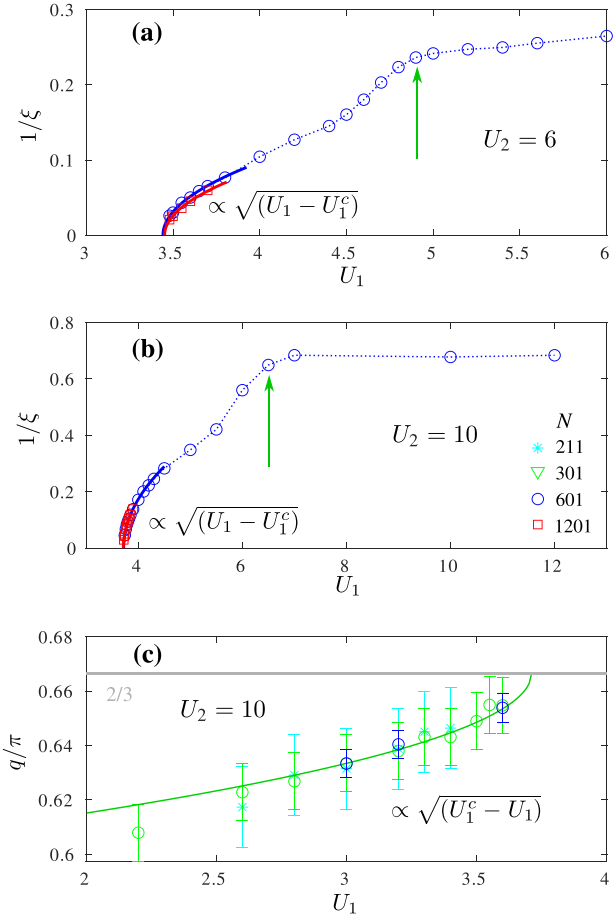

FIG. 7. Additional numerical data across the Pokrovsky-Talapov transition. (a),(b) Inverse of the correlation length upon approaching the transition out of the period-3 phase at (a) $U_2 = 6$ fairly close to the turning point and (b) $U_2 = 10$. Symbols are numerical data, lines are fits with $1/\xi \propto (U_1 - U_1^c)^{\nu}$ with the Pokrovsky-Talapov critical exponent $\nu = 1/2$. One can see the appearance of pronounced kinks inside the period-3 phase. The location of these kinks corresponds to green squares on the phase diagram of Fig. 1. (c) Incommensurate wave-vector q as a function of U_1 upon approaching the Pokrovsky-Talapov transition. Numerical data (symbols) agree with the theory prediction (line) $q - 2\pi/3 \propto (U_1^c - U_1)^{\bar{\beta}}$ with the Pokrovsky-Talapov critical exponent $\bar{\beta} = 1/2$. Green line shows the result of the fit for $N = 301$ with U_1^c being fixed to the value obtained in (b) for $N = 1201$ sites.

What are the consequences of the floating phase and the commensurate-incommensurate Pokrovsky-Talapov transition? First of all, the very fact that Kosterlitz-Thouless transition turns into a Pokrovsky-Talapov transition is surprising and to the best of our knowledge such a possibility has not been reported yet neither in the context of field theory nor in the framework of lattice models. Furthermore, the mismatch between the two critical exponents $K^c_{\rm PT} = 1/9$ and $K^c_{\rm KT} = 2/9$ implies that equal-K lines with $1/9 < K < 2/9$ will condense at the point where the nature of the transition changes as sketched in Fig. 1(b). Qualitatively, slightly convex curvature of the critical line for large U_2 agrees with this picture. However, quantitative verification of this prediction would require much longer chains: such that in the direct vicinity of the Pokrovsky-Talapov transition the chain will host multiple helices to have a reliable fit. Because of strong frustration and low-lying excitations the convergence in the Luttinger liquid phase for large U_2 is extremely slow, while the accuracy required to capture the floating phase must be kept high. This question is left open for future investigations. It would be very interesting and instructive to have insights from the field theory on the nature of the turning point at which the transition changes its nature.

It should be possible to directly program the model of Eq. (1) at one-third filling in optical cavities with individual control over the trapped atoms. This will allow to probe both, the Kosterlitz-Thouless and the Pokrovsky-Talapov transitions experimentally. Also note that the floating phase in the vicinity of the Pokrovsky-Talapov transition, more specifically, the floating phase with the Luttinger liquid parameter $1/9 < K < 1/8$ [29], is stable against a single-particle instability, unlike the rest of the Luttinger liquid phase on the phase diagram. This provides an alternative way to probe the reported-here change of nature of the quantum phase transitions in experiments.

ACKNOWLEDGMENTS

I am indebted to Frédéric Mila for extensive discussions on related projects. I would like to thank The Erwin Schrödinger International Institute for hospitality. This research has been supported by Delft Technology Fellowship. Numerical simulations were performed at the Dutch national e-infrastructure with the support of the SURF Cooperative and Delft High Performance Computing Centre (DHPC).

APPENDIX: ADDITIONAL DATA FOR THE POKROVSKY-TALAPOV TRANSITION

In this Appendix we provide additional data for the Pokrovsky-Talapov transition across the cuts at $U_2 = 6$ [Fig. 7(a)] and at $U_2 = 10$ [Figs. 7(b) and 7(c)]. Along both cuts the correlation length diverges with the Pokrovsky-Talapov critical exponent $\nu = 1/2$. For $U_2 = 10$ one can also compare the data of the incommensurate wave-vector q with theory expectation $q/\pi \propto (U_1^c - U_1)^{\bar\beta}$, where the location of the critical point was extracted by sitting the correlation length as shown in Fig. 7(b) and the critical exponent is fixed to the value of the Pokrovsky-Talapov transition $\bar\beta = 1/2$. For both values of next-nearest-neighbor coupling U_2 one can notice the presence of a crossover deep inside the period-3 phase. We associate the location of the kink (green arrows) with the first point that deviates from the main slope while coming from inside the charge-density wave phase. In Fig. 7(c) we show the incommensurate wave-vector q for $U_2 = 10$ approaching its commensurate value $q = 2\pi/3$ with the critical exponent $\bar\beta = 1/2$. The results agree with those presented in Fig. 6.

[1] T. Giamarchi, *Quantum Physics in One Ddimension*, International Series of Monographs on Physics (Clarendon, Oxford, 2004).

[2] A. M. Tsvelik, *Quantum Field Theory in Condensed Matter Physics*, 2nd. ed. (Cambridge University Press, Cambridge, England, 2003).

[3] S. Sachdev, *Quantum Phase Transitions* (Cambridge University Press, Cambridge, England, 2011).

[4] P. Pfeuty, The one-dimensional ising model with a transverse field, Ann. Phys.(NY) **57**, 79 (1970).

[5] D. A. Huse and M. E. Fisher, Commensurate melting, domain walls, and dislocations, Phys. Rev. B **29**, 239 (1984).

[6] M. den Nijs, The domain wall theory of two-dimensional commensurate-incommensurate phase transitions, Phase Transitions Crit. Phenom. **12**, 219 (1988).

[7] T. Giamarchi, Mott transition in one dimension, Phys. B: Condens. Matter **230**, 975 (1997)

[8] P. Fendley, K. Sengupta, and S. Sachdev, Competing density-wave orders in a one-dimensional hard-boson model, Phys. Rev. B **69**, 075106 (2004).

[9] A. Keesling, A. Omran, H. Levine, H. Bernien, H. Pichler, S. Choi, R. Samajdar, S. Schwartz, P. Silvi, S. Sachdev, P. Zoller, M. Endres, M. Greiner, V. Vuletić, and M. D. Lukin, Quantum Kibble-Zurek mechanism and critical dynamics on a programmable Rydberg simulator, Nature (London) **568**, 207 (2019).

[10] N. Chepiga and F. Mila, Floating Phase versus Chiral Transition in a 1D Hard-Boson Model, Phys. Rev. Lett. **122**, 017205 (2019).

[11] G. Giudici, A. Angelone, G. Magnifico, Z. Zeng, G. Giudice, T. Mendes-Santos, and M. Dalmonte, Diagnosing potts criticality and two-stage melting in one-dimensional hard-core boson models, Phys. Rev. B **99**, 094434 (2019).

[12] D. Poilblanc, S. Yunoki, S. Maekawa, and E. Dagotto, Insulator-metal transition in one dimension induced by long-range electronic interactions, Phys. Rev. B **56**, R1645 (1997).

[13] A. K. Zhuravlev, M. I. Katsnelson, and A. V. Trefilov, Electronic phase transitions in a one-dimensional spinless fermion model with competing interactions, Phys. Rev. B **56**, 12939 (1997).

[14] A. K. Zhuravlev and M. I. Katsnelson, One-dimensional spinless fermion model with competing interactions beyond half filling, Phys. Rev. B **64**, 033102 (2001).

[15] C.-B. Duan and W.-Z. Wang, Bond-order correlation and ground-state phase diagram of a one-dimensional $V_1 - V_2$ spinless fermion model, J. Phys.: Condens. Matter **23**, 365602 (2011).

[16] L. Gotta, L. Mazza, P. Simon, and G. Roux, Pairing in spinless fermions and spin chains with next-nearest neighbor interactions, Phys. Rev. Res. **3**, 013114 (2021).

[17] M. Mattioli, M. Dalmonte, W. Lechner, and G. Pupillo, Cluster Luttinger Liquids of Rydberg-Dressed Atoms in Optical Lattices, Phys. Rev. Lett. **111**, 165302 (2013).

[18] M. Dalmonte, W. Lechner, Z. Cai, M. Mattioli, A. M. Läuchli, and G. Pupillo, Cluster luttinger liquids and emergent supersymmetric conformal critical points in the one-dimensional soft-shoulder hubbard model, Phys. Rev. B **92**, 045106 (2015).

[19] J. Cardy, *Scaling and Renormalization in Statistical Physics*, Cambridge Lecture Notes in Physics (Cambridge University Press, Cambgridge, England, 1996).

[20] P. Di Francesco, P. Mathieu, and D. Sénéchal, *Conformal Field Theory*, Graduate Texts in Contemporary Physics (Springer, New York, 1997).

[21] J. M. Kosterlitz and D. J. Thouless, Ordering, metastability and phase transitions in two-dimensional systems, J. Phys. C **6**, 1181 (1973).

[22] V. L. Pokrovsky and A. L. Talapov, Ground State, Spectrum, and Phase Diagram of Two-Dimensional Incommensurate Crystals, Phys. Rev. Lett. **42**, 65 (1979).

[23] S. R. White, Density Matrix Formulation for Quantum Renormalization Groups, Phys. Rev. Lett. **69**, 2863 (1992).

[24] U. Schollwöck, The density-matrix renormalization group, Rev. Mod. Phys. **77**, 259 (2005).

[25] S. Östlund and S. Rommer, Thermodynamic Limit of Density Matrix Renormalization, Phys. Rev. Lett. **75**, 3537 (1995).

[26] U. Schollwöck, The density-matrix renormalization group in the age of matrix product states, Ann. Phys. (NY) **326**, 96 (2011).

[27] Here we assume open and polarized boundary conditions with $N = 3k + 1$, where $k \in \mathbb{Z}$.

[28] F. C. Alcaraz and R. Z. Bariev, An Exactly Solvable Constrained XXZ Chain, in the *Proceedings of the Conference: Statistical Physics on the Eve of the Twenty-Fist Century* (World Scientific, Singapore, 1999).

[29] R. Verresen, A. Vishwanath, and F. Pollmann, Stable Luttinger liquids and emergent $U(1)$ symmetry in constrained quantum chains, arXiv:1903.09179.

[30] N. Chepiga and F. Mila, Lifshitz point at commensurate melting of chains of rydberg atoms, Phys. Rev. Res. **3**, 023049 (2021).

[31] Higher degree polynomials shows slight signature of overfitting, the difference in the estimated locations of the critical point U_2^c is $O(10^{-3})$.

[32] I. A. Maceira, N. Chepiga, and F. Mila, Conformal and chiral phase transitions in Rydberg chains, Phys. Rev. Res. **4**, 043102 (2022).

[33] R. Samajdar, S. Choi, H. Pichler, M. D. Lukin, and S. Sachdev, Numerical study of the chiral $\mathbb{z}_3$ quantum phase transition in one spatial dimension, Phys. Rev. A **98**, 023614 (2018).